Use of partial load operating conditions for latent thermal energy storage management

Jaume Gasia[1], Alvaro de Gracia[2], Gerard Peiró[1], Simone Arena[3], Giorgio Cau[3], Luisa F. Cabeza[1,*]

[1] GREA Innovació Concurrent, INSPIRES Research Centre, University of Lleida, Pere de Cabrera s/n, 25001, Lleida, Spain

[2] Departament d'Enginyeria Mecanica, Universitat Rovira i Virgili, Av. Paisos Catalans 26, 43007 Tarragona, Spain.

[3] Dept. of Mechanical, Chemical and Materials Engineering, University of Cagliari, Via Marengo 2, 09123, Cagliari, Italy

*Corresponding author: Tel: +34.973.00.35.76. Email: lcabeza@diei.udl.cat

Abstract

A proper management of thermal energy storage (TES) charging and discharging processes allows the final users to optimize the performance of TES systems. In this paper, an experimental research is carried out to study how the percentage of charge in a latent heat TES system (partial load operating conditions) influences the discharge process. Several charging and discharging processes were performed at a constant heat transfer fluid (HTF) mass flow rate of 0.5 kg/s and temperature of 155 ºC and 105 ºC, respectively. High density polyethylene (HDPE) with a total mass of 99.5 kg was used as phase change material (PCM) in a 0.154 m^3 storage tank based on the shell-and-tube heat exchanger concept. Five different percentages of charge have been studied: 63 %, 76 %, 86 %, 92 %, and 97 % (baseline test). Results showed that by modifying the percentage of charge, the time required for the charging process was reduced between 97.2 % and 68.8 % in comparison to the baseline case. However, the energy accumulated was only reduced a maximum of 35.1 % and a minimum of 5.2 %, while the heat transfer rates during the first 60 minutes of discharge were reduced a maximum of 45.8 % and a minimum of 6 %. Therefore, partially charging the TES system not lower than 85% of its maximum energy capacity becomes a good option if the final application accepts a maximum decrease of discharging heat transfer rates of 10% if compared to the fully charged system.

Keywords: Thermal energy storage; Latent heat; Phase change material; Partial load; Thermal management.

Nomenclature

C_p	Specific heat, J/kg·ºC
E	Energy, J
m	Mass, kg
$\dot{m}$	Mass flow rate, kg/s
R	Function which depends on the measured parameters
t	Time, s
T	Temperature, ºC
w	Uncertainties which are associated to the independent parameters
W	Estimated uncertainty in the final result, value-dependent
x	Independent measured parameters

Greek symbols

$\Delta h(T)$	Enthalpy variation (sensible and latent), kJ/kg
ΔT	Temperature variation, ºC

Subscripts

i	Instant
in	Inlet
max	Maximum
n	Control volume
out	Outlet
pr	Process

Abbreviations

DSC	Differential scanning calorimeter
HDPE	High density polyethylene
HTF	Heat transfer fluid
HTR	Heat transfer rate
PCM	Phase change material
RAE	Ratio of accumulated energy
TES	Thermal energy storage
TGA	Thermogravimetry analysis

1 Introduction

Storage technologies, such as thermal energy storage (TES) technologies, have become an indispensable component at any installation coupled to a renewable energy system since they help overcoming the dependence on the weather conditions and the mismatch between energy demands and supplies [1]. A TES cycling process consists of storing the energy when it is available or cheap, but not needed, to further release it when it is demanded and not available or more expensive, with the aim of increasing the efficiency of the thermal process. There are some energy supply sources which are known to be intermittent (i.e. solar energy and industrial waste heat recovery systems) which they might not give a continuous energy supply. Furthermore, if the energy source is able to provide a continuous heat supply, the periodicity of the charge can be adjusted depending on the final demand and the tank design, which is normally not optimized. All these conditions are known as partial load operating conditions and might lead to a TES material which is partially charged and, as a consequence, affect the TES discharging process, especially if the TES material is a phase change material (PCM).

Some of the research work done to study the effect of partial load operating conditions was focused on numerically studying and optimizing the size of sensible cold storage systems for cooling purposes by comparing full storage and partial storage strategies to conventional systems [2-7]. According to Dincer [8], the full storage strategy shifts the entire peak cooling load to off-peak hours, while the partial load strategy is used to either level the load or limit the demand, since the cooling load is partially met by the cooling source and partially met by the storage system. Sebzali et al. [2] studied the effects of using partial and full loads strategies on the TES and chiller size, the reduction of electrical peak demand and the reduction of the energy consumption of a chiller for a clinic building in Kuwait. They found that full storage operation allows larger electrical peak reduction and chiller and storage capacities, while it presents the higher energy consumption. Rahman et al. [3] analysed partial and full TES storage scenarios in a subtropical climate building. Results showed that in both cases more than 50 % of the cooling electricity cost was saved when compared with the conventional system. Macphee and Dincer [4] studied the effect of partial and full storage strategies in the energy and exergy efficiencies of four different types of ice storage techniques for space cooling. They found that both efficiencies were always lower in partial storage systems. Hasnain et al. [5] showed that incorporating partial ice storage systems in Saudi Arabian office buildings reduced the peak electrical power demand and peak cooling load in the up to 20% and up to 40%, respectively. Similarly, Habeebullah [6] performed this analysis for a Saudi Arabian mosque. The author concluded that partial load operating strategies were not economically attractive if compared to full load or conventional systems. Boonnasa and Namprakai [7] performed an optimization of

the payback period for a full load and three different partial load scenarios. They found that partial load scenarios show good economic results as well as manageability and flexibility.

On the other side, literature review showed that some research was also performed to study the influence of partial load operating conditions in latent heat TES systems [9-20]. It is known that when a PCM goes through consecutive melting and solidification processes, it might show specific effects such as hysteresis and/or subcooling. Hence, it might follow different enthalpy-temperature curves for each process (Figure 1a). These effects bring new challenges when numerical models need to evaluate the transition between heating and cooling in TES systems working under partial load operating conditions, since the PCM might have not completely undergone phase change when the following process starts. Four methodologies were found in the literature defining how to address this transition. The first methodology, which was proposed by Bony and Citherlet [9], suggests switching from the heating to the cooling curves, or the other way around, with the same slope than the specific heat curve in the sensible region (points a-c-f in Figure 1b). The second methodology, which was proposed by Rose et al. [10], has the same principle than the first methodology but the transition takes place with no equivalent slope (points a-c'-f in Figure 1b). The third methodology, which was proposed by Chandrasekharan et al. [11], suggests staying at the same curve without considering the other curve (points a-d-f in Figure 1b). Finally, the fourth methodology was obtained in an experimental PCM-equipped wall by Delcroix [12]. He observed that the curve was placed between the cooling and heating curves at a distance and with a slope which depended on the TES system operating conditions (points a-b-e-f in Figure 1b). Palomba et al. [13] experimentally evaluated three short consecutive charging and discharging processes in a latent heat TES system for solar cooling purposes to study the effect of starting a new process without fully melting/solidifying the PCM. They observed that better results could be obtained with longer processes, mainly in the first discharge/charge. Chiu et al. [14] performed a techno-economic optimization of a mobile-TES system in which one of the parameters was the storage level with varying charge/discharge time. Results showed in a monthly base the optimal charge and discharge storage level which provided the maximum economic benefits. Nithyanandam et al. [15] and Zhao et al. [16] numerically analysed the behaviour of packed bed TES systems (with and without encapsulated PCM) under partial load operating conditions in a concentrating solar power plant. Results showed that when the TES system repeatedly worked under partial load conditions, the PCM phase change rate might be limited and the effective storage capacity might be decreased with time. Bedecarrats et al. [17,18] experimentally and numerically investigated the effect of partially discharge a TES system on the following charging process. They observed that the charge mode was relatively shorter and that the subcooling effect practically disappeared. Avignon and Kummert [19] experimentally analysed the effect of

partially charging and discharging a latent heat TES system. They observed that interrupting these processes before the PCM was completely melted or solidified had an effect on the phase change temperature and the degree of subcooling. This effect was also observed in differential scanning calorimeter (DSC) analyses performed by Li et al. [20]. Results showed that the enthalpy-temperature curves of partially melted/solidified PCM were no longer in agreement with the curves obtained in the complete phase change cycles.

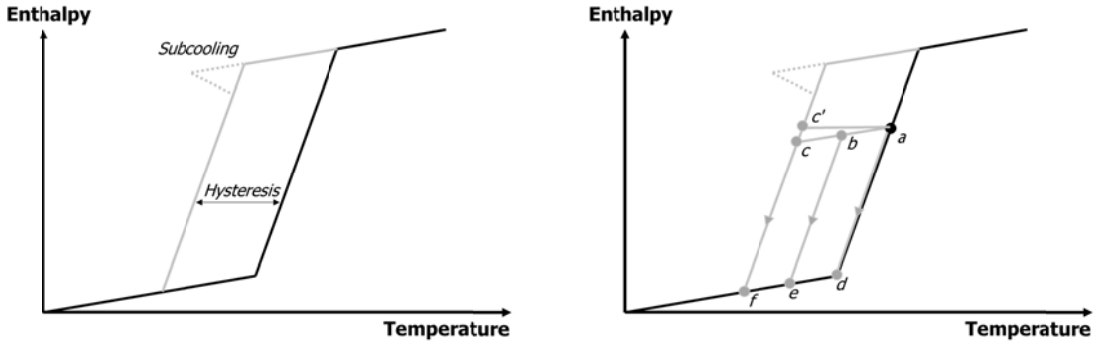

(a) (b)

Figure 1. (a) Hysteresis and subcooling in a PCM melting and solidification process. (b) Scenarios for modelling the transition between heating and cooling in a partially melted PCM. Based on [19].

From the literature review, it was found that little research has been conducted in studying the effect of the partial load operating conditions in a latent heat TES system. Therefore, the aim of the present work is to contribute to fill this gap by experimentally studying and quantifying how the percentage of charge of a latent heat TES system above 100 ºC influences its discharge behaviour. The results presented in this paper provide relevant experimental data to the scientific community which can help to support better sizing decisions, as well as to take into account the greater level of complexity when dealing with latent TES units, as the geometry and operation conditions play a very important role in the heat transfer rates during the melting-solidifying processes.

2 Material, experimental setup and methodology

2.1 Material

The PCM chosen for the present experimentation was high density polyethylene (HDPE) because of its good behaviour in terms of health hazard, thermal stability, and cycling stability [21]. DSC results showed that the melting process occurred between 124 °C and 134 °C, with the melting temperature (peak) at 127 °C, and that the solidification phase change was ranged

between 126 ºC and 114 ºC, with the solidification temperature (peak) at 119 ºC (Figure 2). The methodology used to obtain the enthalpy-temperature and specific heat-temperature curves followed the standard presented in the IEA SHC Task 42 / ECES Annex 29 [22].

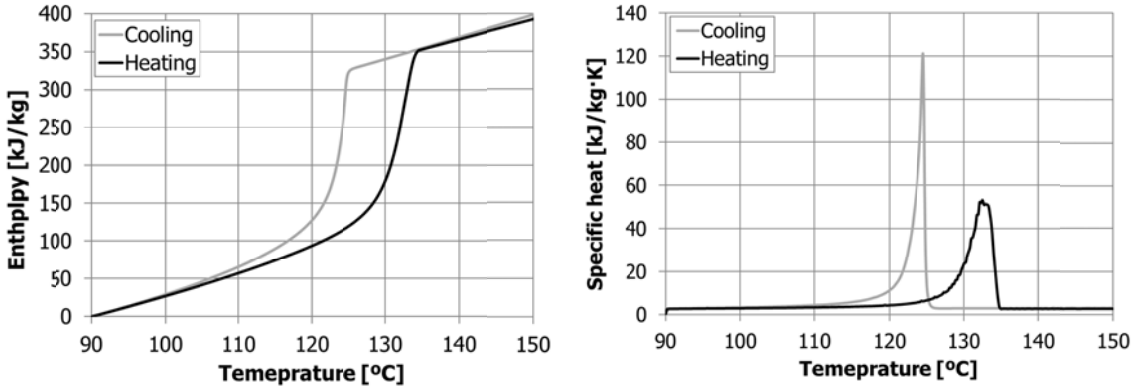

Figure 2. High density polyethylene enthalpy-temperature (a) and specific heat-temperature curves (b) following the PCM standard methodology [22].

2.2 Experimental setup

The experimentation presented in this paper was carried out at the pilot plant facility available at the University of Lleida, which is integrated by three main parts: the heating system, the cooling system, and the storage system. The heating system, which simulates the energy source during the charging process (i.e. solar field, waste heat stream...), consists of a 24 kW_e electrical heater. The cooling system, which simulates the energy consumption, consists of a 20 kW_{th} cross flow air-HTF heat exchanger. Finally, the storage system consists of a stainless steel 304 L storage tank based on the shell-and-tube heat exchanger concept. This design consists of a rectangular prism shaped vessel (0.53 x 0.27 x 1.27 m), where the PCM is located, with a tubes bundle inside containing 49 tubes distributed in square pitch and bended in U-shape, with an average length of 2.49 m (Figure 3a). The capacity of the storage tank is 0.154 m^3 and 99.5 kg of PCM are distributed as shown in Figure 1b: 79% of the PCM is located in the so-called main part, which surrounds the tubes bundle, 14% of the PCM is located in the central part, and finally the remaining 7% is located in the corners. Two Pt-100 1/5 DIN class B temperature sensors, located at the inlet and outlet of the HTF tubes bundle, were used to measure the HTF inlet and outlet temperature ($T_{HTF.IN}$ and $T_{HTF.OUT}$ in Figure 3d) and thirty-one Pt-100 1/5 DIN class B temperature sensors were installed in the storage tank to measure the PCM temperature. Nineteen of these sensors were located in the main part (from $T_{PCM.1}$ to $T_{PCM.15}$ in Figure 3c), six sensors in the corner part close to the U bend (from $T_{c.1}$ to $T_{c.6}$ in Figure 3d), and six in the central part (from $T_{in.1}$ to $T_{in.6}$ in Figure 3d). Each temperature sensor was associated to a control

volume, which is defined as the theoretical volume of PCM in which the value of the temperature sensor could be stated as representative. Six additional Pt-100 1/5 DIN class B where placed on the walls of the storage tank and of the insulation to evaluate the heat losses to the surroundings. The HTF flow rate was measured using a FUJI FCX-A2 V5 series transmitter. Temperature and flow rate sensors were connected to a data acquisition system, which controls, measures and records the information at a time interval of 60 s.

The three above-explained systems are linked through a stainless steel 304 L piping system which distributes the HTF (silicon fluid Syltherm 800) within a flow rate range between 0.3 and 3 m^3/h. The piping system is insulated with rock wool in order to minimize the heat losses to the surroundings.

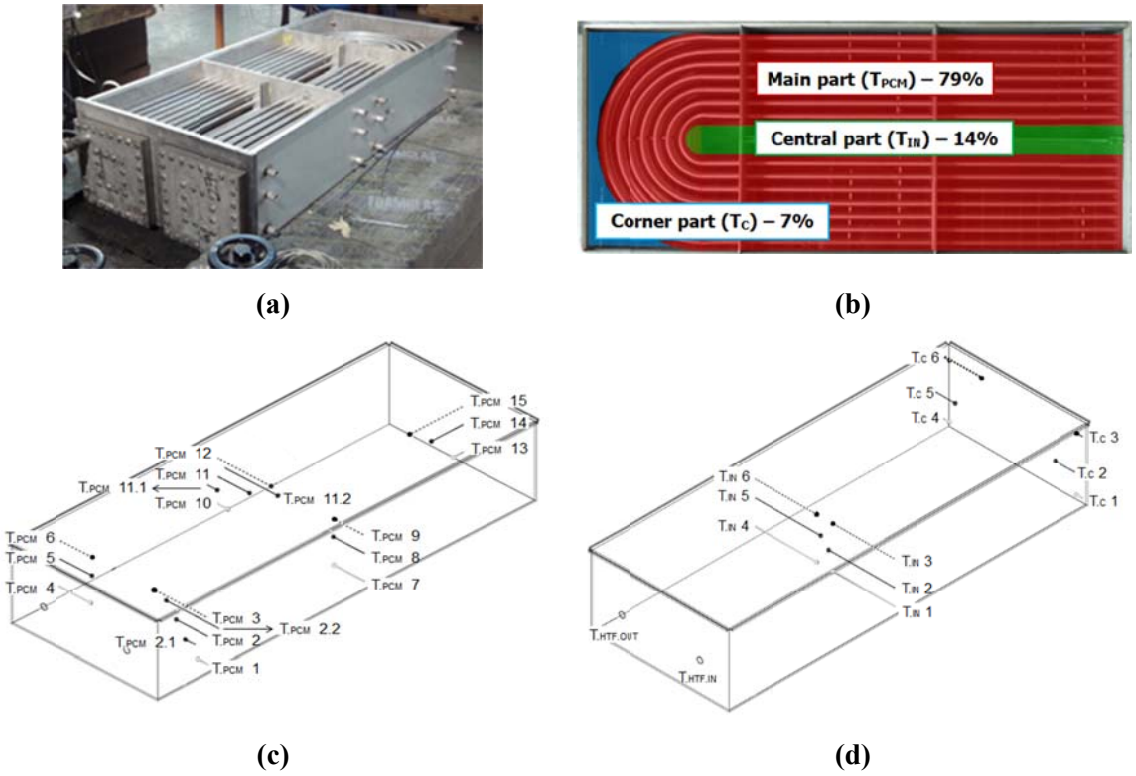

Figure 3. TES system used of the experimental setup: (a) Overview of the TES system; (b) PCM distribution within the TES system; (c) PCM temperature sensors of the main part; (d) Inlet and outlet HTF temperature sensors, and PCM temperature sensors of the corner and central parts.

2.3 Theory and calculation

This section presents the main equations used to describe the experimental results presented in the results and discussion section. The energy stored, or released, by the PCM during the

charging or discharging process, respectively, is calculated as given in Eq. 1. Since HDPE presents hysteresis, the methodology used to study the enthalpy variation under partial load operating conditions followed the one proposed by Chandrasekharan et al. [11], who suggests staying at the same curve without considering the other curve.

$$E_{PCM} = \sum_{n=1}^{27} \sum_{i=1}^{t_{pr}} m_{PCM,n} \cdot \Delta h(T)_{n,(i,i-1)} \quad (1)$$

The heat transfer rate of the HTF during the charging or discharging process is calculated using Eq. 2:

$$\dot{E}_{HTF} = \sum_{i=1}^{t_{pr}} \dot{m}_{HTF} \cdot Cp_{HTF} \cdot (\Delta T_{HTF.in-out}) \quad (2)$$

Finally, the ratio of accumulated energy (RAE), which is the amount of energy accumulated in the PCM at a certain time interval in front of the theoretical maximum energy that can be stored by the PCM is calculated using Eq. 3. The theoretical maximum energy stored was obtained by multiplying the enthalpy variation of the PCM, whose values were acquired from the DSC enthalpy-temperature curves, by the total amount of material used in this experimentation, as described in Eq. 1. In this case, the theoretical maximum energy accumulated by 99.5 kg of HDPE within the temperature range of 105 ºC and 155 ºC is 10.08 kWh. Similarly, the maximum energy stored by the metal parts of the TES system is 1.29 kWh, which is obtained by multiplying their mass by the specific heat of the stainless steel, and by the temperature difference between the initial state and the final state.

$$RAE = \frac{E_{PCM.i}}{E_{PCM.max}} \quad (3)$$

2.4 Methodology

The experimentation presented in this paper consisted of five different charging and discharging tests with the aim of evaluating the effect of partially charging the PCM (partial load operating conditions) on the discharging process (see Table 1). All the processes were carried out using the same parameters, and at least five repetitions of each one were performed to ensure repeatability. Table 1 shows the operating conditions of the partial load charging processes, evaluated by the RAE, and the time needed to reach them. In order to determine the time needed

to reach the evaluated ratios, a 24-hour charging process was carried out. The time needed to reach each RAE was used to control the processes at the pilot plant facility.

Table 1. Operating conditions of the charging processes evaluated in this study

Process	RAE	Time needed to reach this ratio
Charge 1	97 ± 1%	1440 ± 5 min
Charge 2	92 ± 1%	450 ± 3 min
Charge 3	83 ± 1%	150 ± 1 min
Charge 4	73 ± 1%	70 ± 1 min
Charge 5	58 ± 1%	41 ± 1 min

A summary of the flow rates and temperatures used in the experimentation is shown in Table 2. Due to the characteristics of the experimental facility, a homogenization process was required before starting each process, which lasted around 25 minutes for the charging process and 30 minutes for the discharging process. The objective was to ensure a uniformity and homogeneity at both the PCM and HTF initial temperatures shown in Table 2.

Table 2. Summary of the main parameters of the processes.

Process	HTF mass flow rate	HTF inlet temperature	PCM average initial temperature
	[kg/s]	[ºC]	[ºC]
Charge	0.5 ± 0.01	155 ± 2	104 ± 1.5
Discharge	0.5 ± 0.01	105 ± 2	128.5 to 150 (depending on the RAE)

2.5 Uncertainty analysis

This section aims to show the uncertainties of the different parameters and their impact in the results of the present study to determine their precision and general validity. The first step was to establish the uncertainties of the parameters which were measured during the experimentation and the uncertainties associated to the thermophysical properties of the HTF and PCM. These values are shown in Table 3.

Table 3. Uncertainties of the different parameters involved in the analyses of the present study.

Parameter	Units	Sensor	Accuracy
Temperature	ºC	Pt-100 1/5 DIN class B	± 0.3

Flow rate	l/h	FUJI FCX-A2 V5 series transmitter	± 23.7
HTF specific heat	kJ/kg·ºC	From ref. [23]	± 0.054
HTF density	kg/m^3	From ref. [23]	± 25.16
PCM mass	kg	Regular scale	± 0.5
PCM volume	m^3	Storage tank designer	± 0.0024
PCM enthalpy	kJ/kg	Sensors from Mettler Toledo DSC-822e	± 3

Once the uncertainties of these parameters were known, the next step was to estimate the uncertainties of the HTF power and PCM accumulated energy, which were obtained as shown in Eq. 4 [24]. These uncertainties were calculated for each time interval registered.

$$W_R = \left[\left(\frac{\partial R}{\partial x_1}\cdot w_{x_1}\right)^2 + \left(\frac{\partial R}{\partial x_2}\cdot w_{x_2}\right)^2 + \cdots + \left(\frac{\partial R}{\partial x_n}\cdot w_{x_n}\right)^2\right]^{1/2} \quad (4)$$

where W_R is the estimated uncertainty in the final result, R is a function which depends on the measured parameters, x_n are the independent measured parameters, and w_x are the uncertainties which are associated to the independent parameters.

Table 4 shows average uncertainty in HTF power and PCM accumulated energy of the different processes carried out.

Table 4. Estimated uncertainties of the HTF power and PCM accumulated energy.

		Uncertainty of the HTF power [± kW]	Uncertainty of the PCM accumulated energy [± kWh]
RAE	**97%**	0.36	0.064
	92%	0.38	0.063
	83%	0.44	0.042
	73%	0.44	0.042
	58%	0.48	0.049

3 Results and discussion

3.1 Repeatability

Each charging and discharging process was repeated five times to demonstrate repeatability of the methodology and the experimental results. Figure 4 presents the temperature profiles of the HTF at the inlet and outlet of the TES system, and the temperature profiles of the PCM at three different locations (evaluated by the temperature sensors T.PCM.2, T.PCM.5, and T.PCM.14) during the charging and discharging processes for the case study referred to a RAE of 92%. Results from the repeatability tests show that the methodology adopted for the present experimentation produced repeatable values. Notice that only one case study is presented, however, the remaining four case studies also showed repeatability. Moreover, when the phase change temperature range is evaluated in both Figure 2 and Figure 4, slight differences can be observed. On one side, DSC results showed that melting was ranged between 124 ºC and 134 ºC while pilot plant results showed that melting occurred approximately between 127 ºC and 136 ºC. On the other side, DSC results showed that solidification took place between 126 ºC and 114 ºC, while pilot plant results showed that it was ranged between 127 ºC and 124 ºC. The reason for these differences was due to the different heating/cooling rates, different sample masses, which are known to have an influence on the PCM phase change behaviour [25].

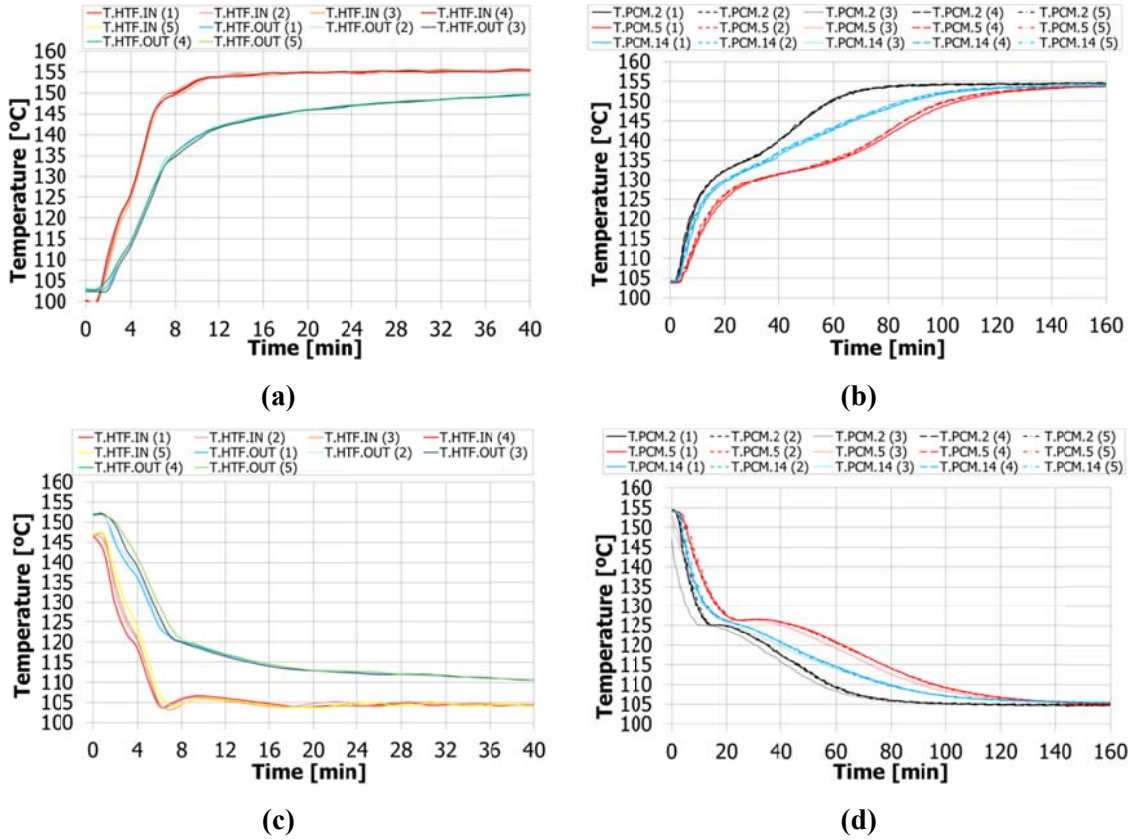

Figure 4. Repeatability tests for the study case of a RAE of 92%: (a) HTF inlet and outlet temperatures during the charging process; (b) PCM temperature at three different locations (evaluated by the temperature sensors T.PCM.2, T.PCM.5, and T.PCM.14) during the charging process; (c) HTF inlet and outlet temperatures during the discharging process; (d) PCM temperature at three different locations (evaluated by the temperature sensors T.PCM.2, T.PCM.5, and T.PCM.14) during the discharging process.

3.2 Charging process

Figure 5 shows the evolution of the time of charge (left axis) and the evolution of the average temperatures of the PCM at the main, corner, and central part of the TES system (right axis) for the different percentages of RAE. These results were used to determine the five case studies presented in this paper. Notice that the profile of the time showed a linear evolution until the RAE achieved the value of 55%. From this value to a value of RAE of 70%, the time profile also showed a linear evolution but with a different slope, which indicates that the time needed to increase the RAE is increased. Finally, from the value of RAE of 70% up to the maximum achievable RAE (in the present study this value was 97% after 24 h, which was limited because of the current geometrical design of the TES system and the existing heat losses), the time profile showed a non-linear evolution, since the efforts were focused on melting the PCM located on the corner part and on increasing the temperature of the already liquid PCM.

A more detailed profile time study is shown in Figure 6. This figure shows the time needed to increase 5% the value of the RAE during the charging process (notice that the primary and secondary y-axes are in a log-2 scale). It can be observed that for the first period (from 0% to 55%) the time needed was five minutes or less. Specifically, it can be seen that the time to store the initial 5% of energy was slightly higher than the time needed to increase the following 5% until a RAE of 55%. The reason is due to two factors. On one hand, during the first six minutes of charge, the heat transfer gradually increases from 0 to its maximum, as seen in Figure 7, and as a consequence, the energy transferred in this period is lower. On the other hand, part of this energy is absorbed initially by the metal of the tubes bundle and afterwards by the PCM located around it in terms of sensible energy. After the first 5%, it takes between two and four minutes to increase 5% until the ratio of energy accumulated (RAE) is 55%. On the other hand, in the second period (from 55% to 70%) the required time was at least nine minutes. Finally, the time needed to increase 5% the RAE in the third period (from 70% to 97%) increased exponentially. As explained above, the main reason for this behaviour is that when the RAE achieved the value of 70% the PCM located at the main and central parts was already melted. Therefore, the biggest amount of energy from the HTF was focused on increasing the temperature and melting the PCM located at the corner part. The existing distance between the corners and the HTF tubes bundle, and the low thermal gradient between the PCM and the HTF induced low heat transfer rates and a reduction in the power of energy absorbed by the PCM. The existence of this non-linear profile from the RAE of 70% shows the potential of using partial load operating conditions when a fast charging process needs to be performed, mainly because of the heating source availability.

If the different case studies are compared to the baseline case study (RAE 97%), different reductions on the energy accumulated at the end of the charging process and the time needed to reach these levels are observed. In the case study of RAE 92%, a reduction of 5.2% of the accumulated energy, which causes a time reduction of 68.8% on the charging period. This variation on the charging time is even increased in the other case studies. If the accumulated energy is reduced 14.4% (RAE 83%), 24.7% (RAE 73%), and 40.2% (RAE 58%), the period of time needed to reach these levels is reduced 89.6%, 95.1%, and 97.2%, respectively (Table 5).

Focusing again on the temperature profiles shown in Figure 5, it can be seen that the baseline study case (cross mark) shows always higher temperature in the three different regions than the other case studies as a result of the higher amount of accumulated energy. Looking at the PCM distribution in the TES system, it can be seen that the average temperature of the PCM located in the main part at the end of the charging process, in comparison to the baseline case study, has

a temperature variation which goes from 12.8% in the case of RAE 58% (round mark) to a difference of only 0.4% in the case of RAE 92% (rhombus mark). Observing the PCM located in the central part, the temperature variation compared to the baseline study case goes from the 19.8% in the case of RAE 58% to 3.5% in the case of RAE 92%. Finally, the PCM located in the corners of the TES system, shows a higher temperature variation, from 25.4% in the study case of RAE 58% to 6.5% in the case of RAE 92%. These results show that, if compared to the baseline study case, the PCM located at the main part presents a lower temperature variation than the PCM located in both the central and corner parts. The reason lies on the fact that this PCM surrounds the HTF tubes bundle and therefore it received first the heat released by the HTF and it increased faster its temperature. Moreover, Figure 5 shows that the PCM located in the corners of the TES system did not fully melt. This was mainly caused by a non-optimized design of the TES system, which creates dead zones. Hence, the effect of the heat losses was higher than the effect of the heat transfer from the HTF.

Figure 7 presents the evolution of the HTF heat transfer rate during the charging process of the five study cases. These profiles are limited to 180 minutes for a better visualization. As expected, the heat transfer rates are practically the same for the different studies until they are stopped, and the slight variations are due to the small variations on the initial conditions and mass flow rates. These profiles show an exponential behaviour with significantly higher values during the first 10 minutes of process, when the heat is mainly transferred to the metal tubes bundle, and therefore rapidly increases its temperature, and when the thermal gradient between the HTF and the PCM is maximum. Afterwards, while the PCM increases its temperature, the values of the heat transfer exponentially decrease until minimum values. At this moment, the heat transfer is focused on increasing the temperature of the PCM located at the corners and the central part of the tank.

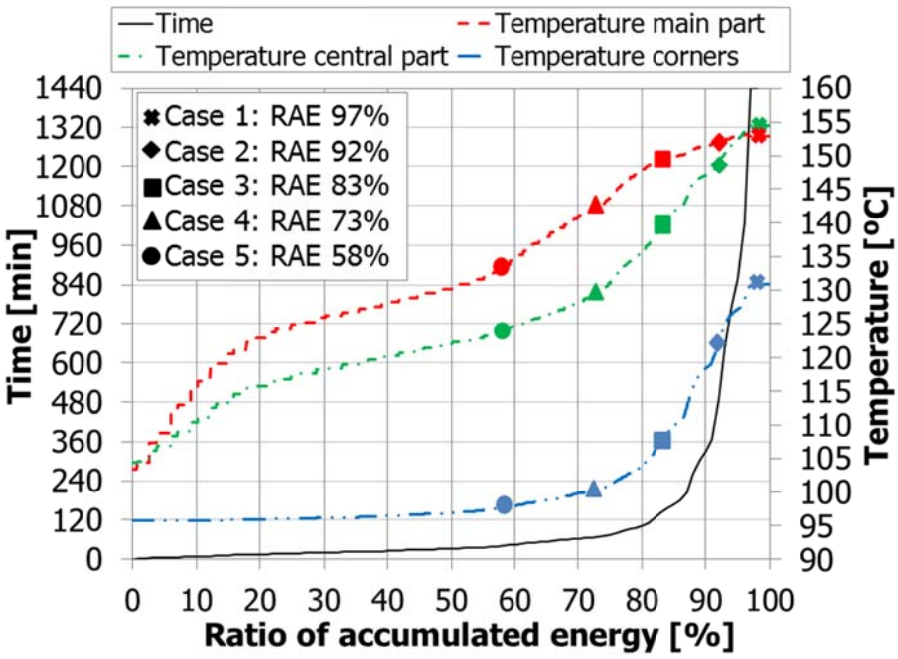

Figure 5. Evolution of the time during a charging process (left-y axis) and evolution of the temperature of the PCM in the main, central, and corner parts of the TES system (right-y axis) according to the ratio of accumulated energy (RAE) of the charging process.

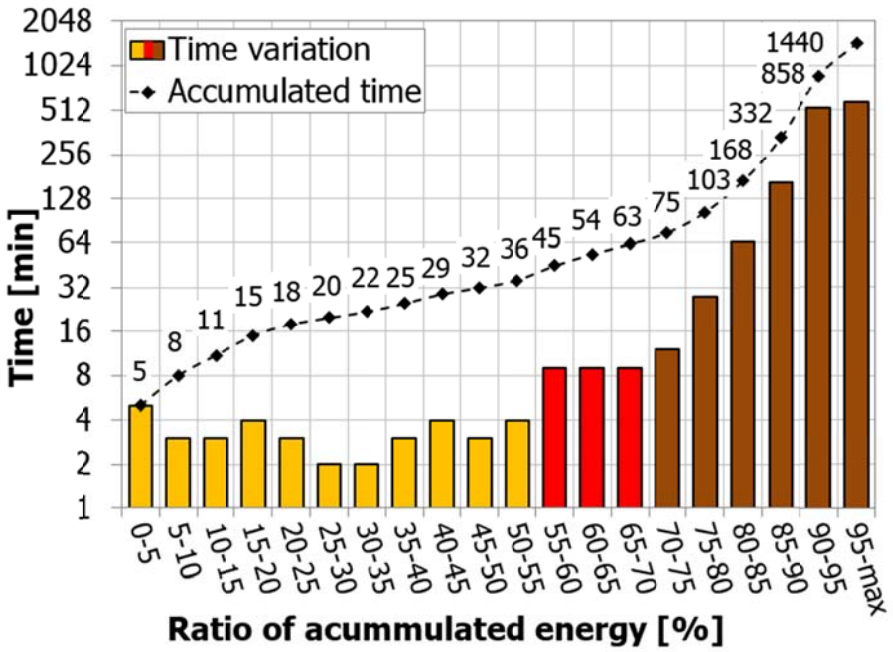

Figure 6. Time variation needed to increase 5% the energy accumulated in the studied TES system for a 24-hour charging process (bars) and accumulated time during this (line) the same charging process.

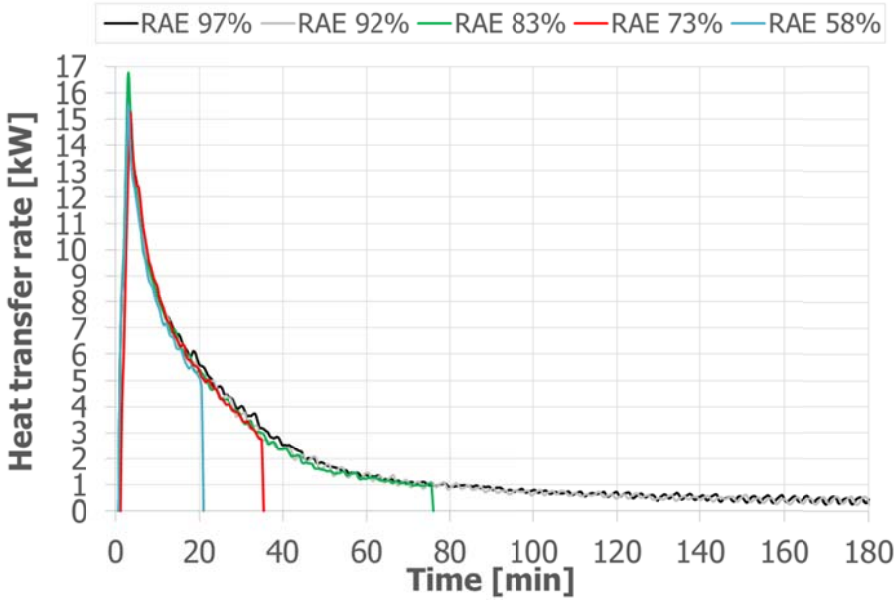

Figure 7. Evolution of the HTF heat transfer rate during the charging processes of the five study cases presented in this study.

3.3 Discharging process

In order to study the influence that the RAE during the charging process has on the discharging process, the authors decided to analyse the temperatures and heat transfer rates. Figure 8 shows the evolution of the PCM temperature during the discharging process at the three characteristic locations of the storage tank, as well as the weighted average temperature of the whole PCM, for the five case studies. For the whole discharging processes, higher temperatures were observed for the study cases with a higher RAE, no matter where the PCM was located. However, an interesting phenomenon could be observed in the PCM located at the corners (Figure 8d). During the first 40-90 minutes of the discharging process, depending on the RAE during the charging process, the average temperature of the PCM slightly increased since the energy transferred from the PCM located at the main part was higher than the energy lost through the walls. After this period, the PCM temperature started to decrease for opposite reasoning.

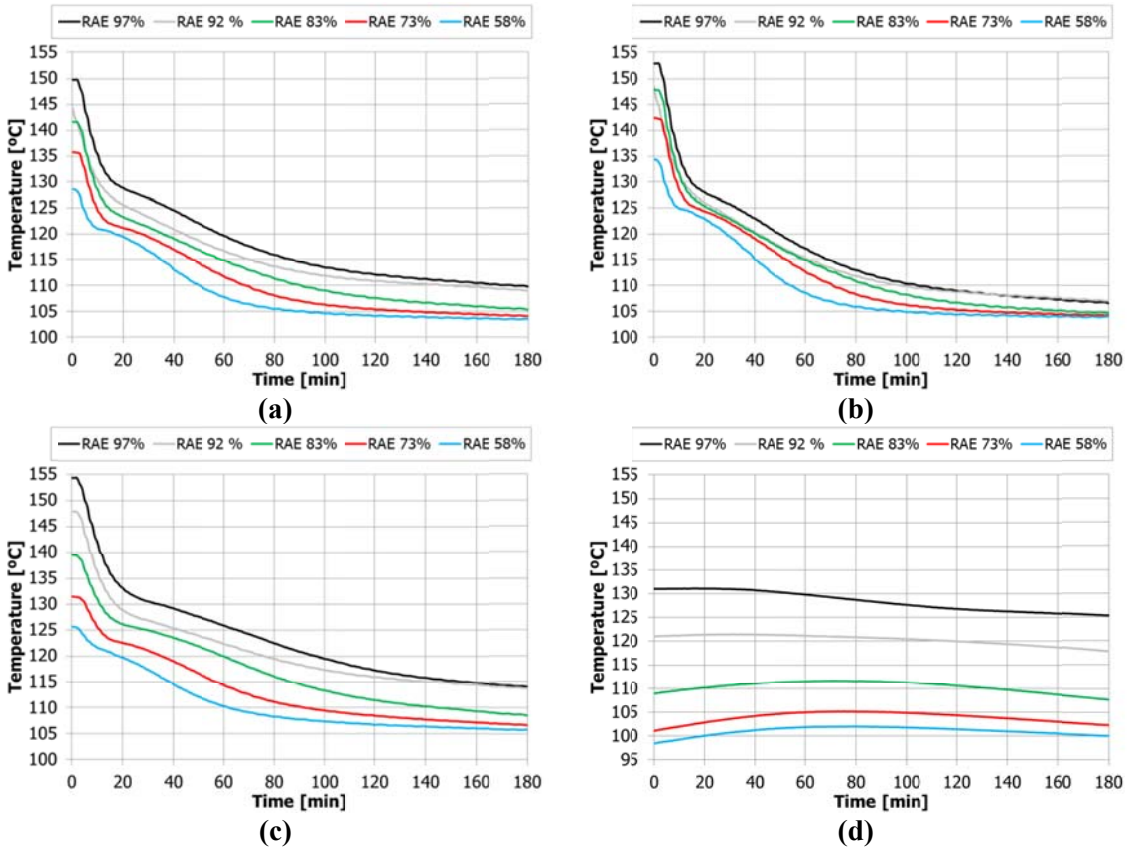

Figure 8. Evolution of the weighted average PCM during the discharging process: (a) All control volumes; (b) Control volumes located at the main part; (c) Control volumes located at the central part; (d) Control volumes located at the corners.

The evolution of the HTF temperature at the outlet of the HTF tubes bundle for the different RAE is presented in Figure 9. Notice that only the first 180 minutes are presented for a better comprehension of the readers since the values for longer periods of time present an asymptotic trend. Results in Figure 9 show that the HTF outlet temperature during the discharging process is clearly affected by the percentage of charge. It is observed that the outlet HTF temperature decreased as the RAE during the charge decreased and the variations in comparison to the baseline study case were higher when the RAE during the charge were 73% and 58%. Due to the fact that both the inlet HTF temperature and mass flow rate were kept almost constant along the different discharging processes, the heat transfer rates were also affected similarly than the outlet HTF temperature as shown in Figure 10. Figure 11 goes a step further and numerically quantifies the average values of the heat transfer rates every 30 min from the beginning to the minute 180. Results show that during the first 30 minutes the heat transfer rates of all the case studies, except for the case study RAE 58%, presented a variation, compared to the baseline case, lower than 10% (Table 5). During the next 30 minutes only the RAE 92% and RAE 83% kept average heat transfer rates with a variation, compared to the baseline case, lower than 10 %. From this period on, all the case studies presented variations higher than 10%. Therefore, it

can be concluded that if the TES system is required to supply thermal energy for a short period of time (i.e. discharging process of less than 60 min) the penalization of working under partial load operating conditions during the charging process are widely overcome by the charge time reductions, mainly in the cases of RAE 92% and 83%. Finally, a comparison of the heat transfer rates during the discharging process for the five case studies when the PCM accumulated energy reached the same value than the energy stored at the beginning of the study case of RAE 58% is presented in Figure 12. This state was achieved after 34 minutes (RAE 97%), 22 minutes (RAE 92%), 20 minutes (RAE 83%), and 14 minutes (RAE 73%) of starting their respectively discharging processes. It can be observed that the heat fluxes are not the same, which indicates the influence of the PCM temperature distribution within the TES system on the heat transfer rates during the discharging process. The PCM was already solidified around the tubes bundle in the case of RAE 97%, 92%, 83%, and 73% since the weighted average temperature in all cases was around 125 ºC. However, in the case study of RAE 58%, the PCM around the tubes bundle was still liquid since it was the beginning of the process. As a consequence, the driving force between the PCM and the HTF, and the thermal resistance around the tubes bundle greatly affected the heat transfer rates.

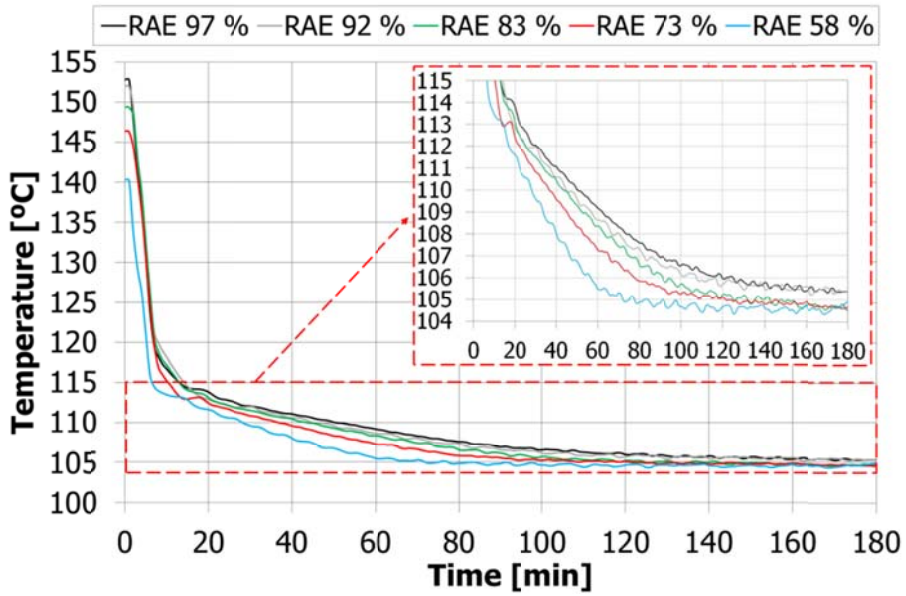

Figure 9. Evolution of the outlet HTF temperature during the discharging processes of the five study cases presented in this study.

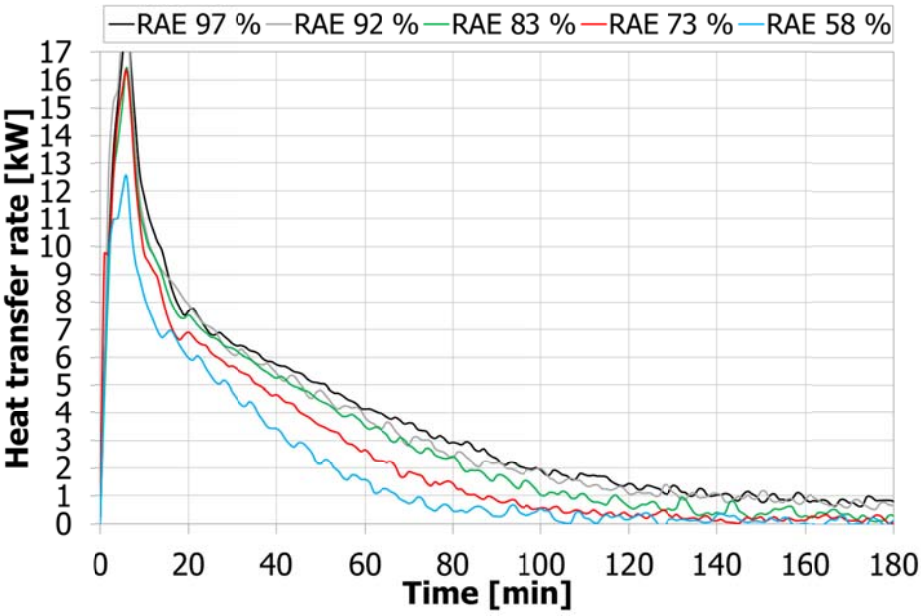

Figure 10. Evolution of the HTF heat transfer rate during the discharging processes of the five study cases presented in this study.

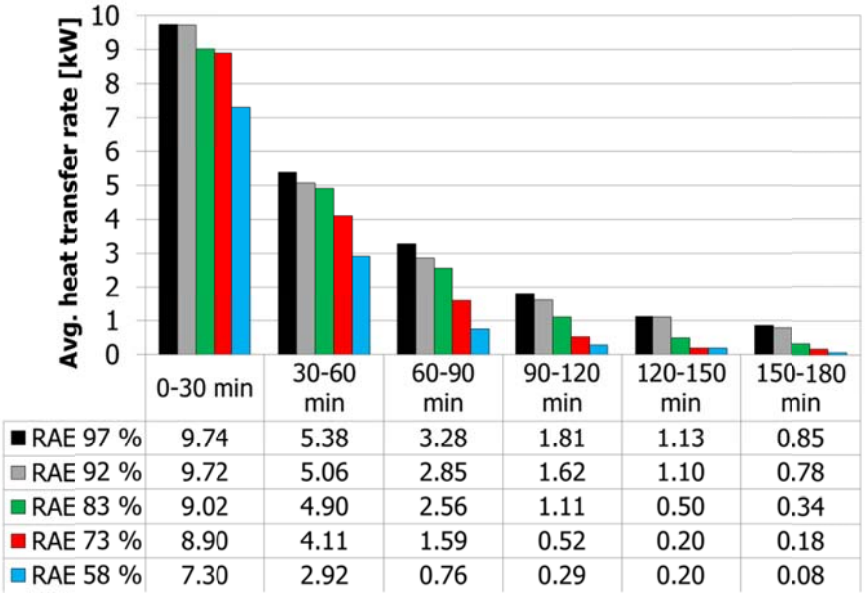

	0-30 min	30-60 min	60-90 min	90-120 min	120-150 min	150-180 min
RAE 97 %	9.74	5.38	3.28	1.81	1.13	0.85
RAE 92 %	9.72	5.06	2.85	1.62	1.10	0.78
RAE 83 %	9.02	4.90	2.56	1.11	0.50	0.34
RAE 73 %	8.90	4.11	1.59	0.52	0.20	0.18
RAE 58 %	7.30	2.92	0.76	0.29	0.20	0.08

Figure 11. Evolution every 30 min of the averaged HTF heat transfer rate during the discharging processes of the five study cases presented in this study.

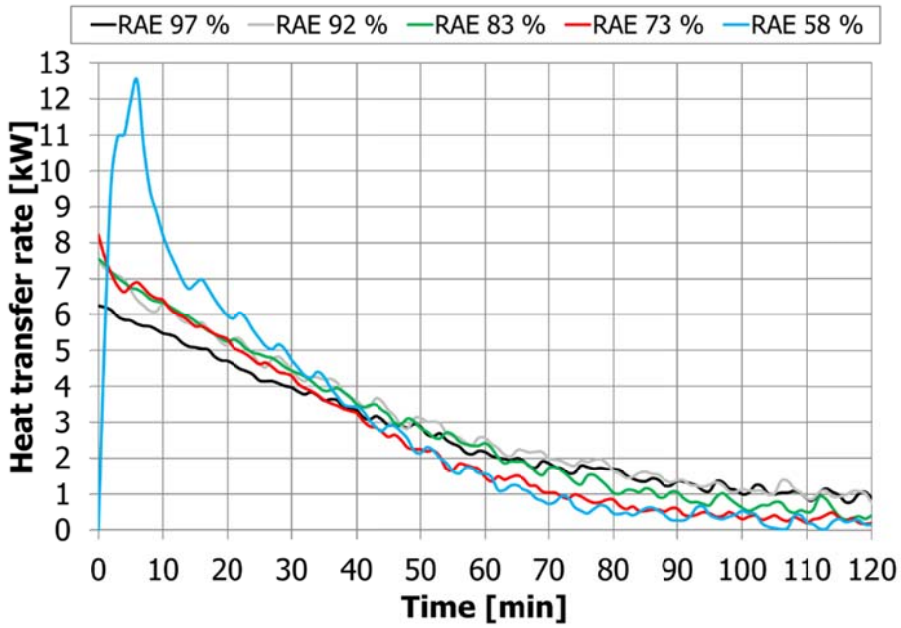

Figure 12. Evolution of the HTF heat transfer rate during the discharging processes of the five study cases when the accumulated energy is 58%. Notice that 0 in the "x" axis means the moment when the different study cases achieved this value, and not the beginning of the discharging process.

Table 5. Summary of the variation of the main results discussed in the present paper compared to the baseline case (RAE 97 %).

		Charge		**Discharge**					
		Δ RAE	**Δ Process time**	**Δ Average HTR* 0-30 min**	**Δ Average HTR 30-60 min**	**Δ Average HTR 60-90 min**	**Δ Average HTR 90-120 min**	**Δ Average HTR 120-150 min**	**Δ Average HTR 150-180 min**
RAE	**97 %**	-	-	-	-	-	-	-	-
	92 %	5.2 %	68.8 %	0.3%	6.0%	13.3%	10.7%	2.7%	7.9%
	83 %	14.4 %	89.6 %	7.4%	9.0%	22.1%	38.5%	55.8%	59.8%
	73 %	24.7 %	95.1 %	8.7%	23.7%	51.5%	71.3%	82.3%	78.4%
	58 %	40.2 %	97.2 %	25.0%	45.8%	76.8%	84.2%	82.3%	91.0%

*HTR: Heat transfer rate

4 Conclusions

The work presented in this paper studies how the fact of partially charging a latent heat TES system influences the discharging process (partial load operating conditions). Five different percentages of charge were studied and discussed, which were determined with a 24-hour charging process. The parameter ratio of accumulated energy (RAE) was defined to evaluate the partial load charging processes. This ratio defines the PCM accumulated energy at a certain time interval in front of the theoretical maximum energy stored by the PCM. The five case studies were RAE 97 %, RAE 92 %, RAE 83 %, RAE 73 %, and RAE 58 %, being the first one the baseline case.

The experimental results showed that during the charging process, the evolution of the time according to the RAE presented three different profiles. From the beginning to a RAE of 55%, the profile of the time showed a linear evolution. After this value to a RAE of 70%, the time profile also showed a linear evolution but with a different slope. Finally, from the value of RAE of 70% up to the maximum achievable RAE (97%) the time profile showed a non-linear evolution. Moreover, it was observed that in comparisons to the baseline case, by reducing the RAE between 5.2% and 40.2%, the charging process time could be reduced between 68.8 % and 97.2%. Therefore, in terms of time, working under partial load operating conditions is beneficial. However, during the discharging process partial load operating conditions penalize the heat transfer rate. Before the first hour of discharge, only the case studies of RAE 92% and 83% showed heat transfer rates values which were 10% lower than the baseline case, and after the first hour all the case studies present a reduction on the heat transfer rates in comparison to the baseline case higher than 10%. Therefore, if the TES system works under partial load operating conditions during the charging process for a RAE higher than 83%, it is able to supply heat transfer rates during the first 60 min of the discharging process with variations lower than 10% compared to the baseline case, but with significant time reductions in the charging process of more than 89%.

Finally, it has to be pointed out that the results presented in this paper are strongly affected by the particular geometry of the system, which presents two dead zones (at the corners) that cannot be effectively used. Different geometries, with different distribution of tubes or different container shapes, could yield different results.

Acknowledgements

The work was partially funded by the Spanish government (ENE2015-64117-C5-1-R (MINECO/FEDER), ENE2015-64117-C5-3-R (MINECO/FEDER), and ULLE10-4E-1305). The authors would like to thank the Catalan Government for the quality accreditation given to their research group (2014 SGR 123). GREA is certified agent TECNIO in the category of technology developers from the Government of Catalonia. This project has received funding from the European Commission Seventh Framework Programme (FP/2007-2013) under Grant agreement Nº PIRSES-GA-2013-610692 (INNOSTORAGE) and from the European Union's Horizon 2020 research and innovation programme under grant agreement No 657466 (INPATH-TES). Jaume Gasia would like to thank the Departament d'Universitats, Recerca i Societat de la Informació de la Generalitat de Catalunya for his research fellowship (2017 FI_B1 00092). Alvaro de Gracia would like to thank Ministerio de Economia y Competitividad de España for Grant Juan de la Cierva, FJCI-2014-19940. Simone Arena would like to thank the Department of Mechanical, Chemical and Materials Engineering of the University of Cagliari for funding his research grant.

References

1. H. Mehling, LF. Cabeza, Heat and cold storage with PCM. An up to date introduction into basics and applications. Berlin, Germany. Springer-Verlag 2008. ISBN: 979-3-540-68556-2.
2. M. Sebzali, P. Rubini, Analysis of ice cool thermal storage for a clinic building in Kuwait, Energy Conversion and Management, 47 (2006) 3417–3434.
3. M. Rahman, M. Rasul, M. Khan, Feasibility of thermal energy storage systems in an institutional building in subtropical climates in Australia, Applied Thermal Engineering, 31 (2011) 2943–2950.
4. D. Macphee, I. Dincer, Performance assessment of some ice TES systems, International Journal of Thermal Sciences, 48 (2009) 2288–2299.
5. SM. Hasnain, SH. Alawaji, AM. Al-Ibrahim, MS. Smiai, Prospects of cool thermal storage utilization in Saudi Arabia, Energy Conversion and Management, 41 (2000) 1829–1839.
6. BA. Habeebullah, Economic feasibility of thermal energy storage systems, Energy and buildings, 39 (2007) 355–363.
7. S. Boonnasa, P. Namprakai, The chilled water storage analysis for a university building cooling system, Applied Thermal Engineering, 30 (2010) 1396–1408.
8. I. Dincer, On thermal energy storage systems and applications in buildings, Energy and Buildings 34 (2002) 377–388.

9. Bony, S. Citherlet, Numerical model and experimental validation of heat storage with phase change materials, Energy Buildings, 39 (2007) 1065–1072.
10. J. Rose, A. Lahme, N.U. Christensen, P. Heiselberg, M. Hansen, K. Grau. Numerical method for calculating latent heat storage in constructions containing phase change material. In Proceedings of Building Simulation 2009: 11th Conference of the International Building Performance Simulation Association, 400–407. Glasgow, Scotland, GBR, July 27–30.
11. R. Chandrasekharan, E.S. Lee, D.E. Fisher, P.S. Deokar. An enhanced simulation model for building envelopes with phase change materials, ASHRAE Trans, 119 (2013).
12. B. Delcroix. Modelling of Thermal Mass Energy Storage in Buildings with Phase Change Materials. PhD dissertation, Department of Mechanical Engineering, École Polytechnique de Montréal, Montréal, QC, Canada (2015).
13. V. Palomba, V. Brancato, A. Frazzica. Experimental investigation of a latent heat storage for solar cooling applications Applied Energy, 199 (2017) 347-358.
14. JN. Chiu, J. Castro Flores, V. Martin, B. Lacarrière, Industrial surplus heat transportation for use in district heating, Energy, 110 (2016) 139–147.
15. K. Nithyanandam, R. Pitchumani, A. Mathur, Analysis of a latent thermocline storage system with encapsulated phase change materials for concentrating solar power, Applied Energy, 113 (2014) 1446–1460.
16. B. Zhao, M. Cheng, C. Liu, Z. Dai, Cyclic thermal characterization of a molten-salt packed-bed thermal energy storage for concentrating solar power, Applied Energy, 195 (2017) 761-773.
17. J.P. Bédécarrats, J. Castaing-Lasvignottes, F. Strub, J.P. Dumas. Study of a phase change energy storage using spherical capsules. Part I: Experimental results. Energy Conversion and Management 50 (2009) 2527–2536.
18. J.P. Bédécarrats, J. Castaing-Lasvignottes, F. Strub, J.P. Dumas. Study of a phase change energy storage using spherical capsules. Part II: Numerical modelling. Energy Conversion and Management 50 (2009) 2537–2546.
19. K. D'Avignon, M. Kummert. Experimental assessment of a phase change material storage tank. Applied Thermal Engineering 99 (2016) 880–891.
20. L. Li, H. Yu, X. Wang, S. Zheng. Thermal analysis of melting and freezing processes of phase change materials (PCMs) based on dynamic DSC test. Energy and Buildings 130 (2016) 388–396.
21. J. Gasia, M. Martin, A. Solé, C. Barreneche, LF. Cabeza, Phase change material selection for thermal processes working under partial load operating conditions in the temperature range between 120 ºC and 200 ºC, Applied Sciences, 7 (2017) 722.

22. S. Gschwander, T. Haussmann, G. Hagelstein, A.Sole, G. Diarce, W. Hohenauer, D. Lager, C. Rathgeber, P. Hennemann, A. Lazaro, H. Mehling. Standard to determine the heat storage capacity of PCM using hf-DSC with constant heating/cooling rate (dynamic mode), DSC 4229 PCM Standard. A technical report of subtask A2.1 of IEA SHC 42 / ECES Annex 29 (2015).
23. H. Benoit, D. Spreafico, D. Gauthier, G. Flamant, Review of heat transfer fluid in tube – receivers used in concentrating solar thermal systems: Properties and heat transfer coefficients, Renewable Sustainable Energy Reviews, 55 (2016) 298–315.
24. J.P. Holman, Experimental Methods for Engineers, eight ed. McGrawHill, Newyork (2012).
25. H. Mehling, C. Barreneche, A. Solé, L.F. Cabeza. The connection between the heat storage capability of PCM as a material property and their performance in real scale applications. Journal of Energy Storage 13 (2017) 35–39.